TITLE:

Detrital Zircons from the Amazon river-to-fan system reveal base level controls on land-to-sea sediment transfer

AUTHORS

[1]Cody C. Mason, [1]Brian W. Romans, [2]Daniel F. Stockli, [3]Russel W. Mapes, and [4]Andrea Fildani

[1]Department of Geosciences, Virginia Tech, 4044 Derring, Blacksburg Virginia, 24060, USA

[2]Department of Geological Sciences, The University of Texas at Austin, 1 University Station C1100, Austin, Texas 78712, USA

[3]ExxonMobile, 22777 Springwoods Village Pkwy, Spring, Texas 77389 USA

[4]Statoil Research Center, Austin, Texas 78730, USA

KEYWORDS

Amazon Fan, Amazon River, Sediment Routing System, Detrital Zircons, Sea Level, Climate Change

ABSTRACT

Large tropical sediment routing systems have relatively stable output fluxes over observable timescales. However, the functioning of sediment transfer in these systems across Pleistocene climate and sea-level fluctuations is not well documented. Here, we use new U-Pb detrital zircon (DZ) geochronology from the Pleistocene Amazon submarine fan (n=1,362 grains) to investigate provenance signatures through space and time in Earth's largest source-to-sink system (~$7x10^6$

km^2 onshore). DZ U-Pb ages from the Amazon River system display a progressive downstream dilution of Phanerozoic zircons by older cratonic zircons, predicting a submarine fan with significant proportions of craton-derived sediment. Rather than resembling DZ distributions of the lowest reaches of the Amazon, the well-mixed DZ signature of the Pleistocene submarine fan is nearly identical to an integrated Holocene Amazon system. We hypothesize that base level (sea level) is a first-order control on spatiotemporal patterns of DZ ages in the river and submarine fan: during higher sea level, the Amazon system experiences efficient sediment trapping in its lower reaches. During lower sea levels, the Amazon responds with incision and an increased gradient, resulting in reduced onshore to coastal sediment retention, channel lengthening, and enhanced throughput of Andean derived DZs to the deep sea. We speculate that this phenomenon may influence DZ compositions in other river to submarine fan systems globally.

INTRODUCTION

The responses of linked fluvial to deep-sea sedimentary systems to climate and sea-level fluctuations over multi-millennial timescales are complex and nonlinear (Blum and Törnqvist, 2000). Early and influential research on major fluvial systems focused on the role of base level (sea level) in the context of climate change (Fisk, 1944), while subsequent research modified conceptual models in recognition of the influence of up-stream climate modulated sediment supply and hydrology (Saucier, 1996). Other studies have considered the controls on the timing of submarine fan activity (Covault and Graham, 2010; Maslin, 2009), sediment caliber and volumes delivered to submarine fans (Sweet and Blum, 2016), as well as sediment exhumation and transit rates and the role of river avulsions in sediment transfer to the deep sea (Blum et al.,

47 2018). We consider modern provenance techniques from major river-to submarine fan systems to
48 be a valuable and underutilized tool in the ongoing debate regarding the controls on sediment
49 routing system behavior over multi-millennial timescales.

50 Continent-scale rivers transfer immense loads of solutes and solids to Earth's oceans
51 (Milliman and Farnsworth, 2011), and the Amazon River and deep-sea fan represent a globally
52 important end member for understanding land-to-sea sediment dynamics. Submarine fans have
53 been shown to archive histories of output fluxes and onshore environmental change (Normark
54 and Reid, 2003; Fildani et al., 2016). Fluctuations of sediment sources through time have been
55 inverted from submarine fans and related to up-system climate forcings in linked continent-scale
56 rivers (Clift et al., 2008; Fildani et al., 2016; Mason et al., 2017). The Amazon catchment has
57 distinct sediment and DZ source terranes and physiography (Fig. 1), and the modern onshore
58 fluvial system is characterized by published DZ U-Pb data (Fig. 1B) (Mapes, 2009; Iizuka,
59 2010), constraining patterns of Holocene sediment sources and mixing. A robust record of DZ
60 provenance from the Pleistocene submarine fan should offer new insights into the functioning of
61 this major tropical system in the context of fluctuating climate and sea levels.

62 We present 1,362 new U-Pb DZ ages from 10 samples from cores recovered in the deep-
63 sea Amazon Fan (Sites 936, 945, 946) during Ocean Drilling Program (ODP) Leg 155, in order
64 to explore spatiotemporal patterns of sediment provenance. We integrate our results with
65 published U-Pb DZ data from the modern onshore Amazon fluvial system to elucidate the role of
66 climate and sea level on sediment dynamics over multi-millennial timescale within Earth's
67 largest fluvial to deep-sea sediment routing system.

68

69 **THE AMAZON SOURCE-TO-SINK SYSTEM**

The Amazon River represents Earth's largest fresh water discharge to the ocean (15 – 20% of global total) and largest total sediment load (~1200 Mt yr^{-1}), and is the largest fluvial system in terms of drainage basin area (~$7x10^6$ km^2) (Milliman and Farnsworth, 2011). Acoustic surveys of buried Amazon River and major tributary channels show that incision during the last glacial maximum (LGM) significantly altered the elevation and slope of the river bed (*i.e.* from ~0.7 to ~7 cm/km) (Müller, 1995; Mertes and Dunne, 2007). The degree of upstream propagation of incision is debated, but incision affected bed elevations at the confluence of the Negro (Fig. 1A), and may have propagated as far as 1700 km from the modern coast (Mertes and Dunne, 2007 and references therein).

The lower reaches of the modern Amazon River are significantly influenced by backwater and tidal effects (>1000 km from the river mouth), which in turn also influences backwater effects of its major tributaries (Meade et al., 1991). Sediment budgets indicate only 4 – 5% of sediment shed from the Andes reaches the modern continental shelf (Aalto, 2006), demonstrating the enormous sediment trapping and storage capacity in the modern Amazon system. Cosmogenic radionuclide concentrations from modern fluvial sediments show significant durations (~10^6 yr) of burial and recycling, while cosmogenic radionuclide derived denudation rates result in sediment yields that agree (within a factor of ~2) with decadal timescale direct measurements, indicating the Amazon system is potentially capable of buffering 10^3-10^5 yr signals of climate change (Wittmann et al., 2011).

The Amazon River delta is heavily sculpted by waves and tides and expressed as subaqueous clinoforms that shape the modern continental shelf (Nittrouer et al., 1986). The submarine fan is late Miocene through Pleistocene in age and up to ~4 – 5 km thick (Figueiredo et al., 2009). Accumulations of mainly terrigenous siliciclastic sediment are fed by a canyon

point source, and constructed by multiple channel-levee complexes that terminate in horizontally stratified submarine fan lobes (Damuth et al., 1995). Sedimentation on the fan occurs when eustatic sea levels are >50 m below late Holocene levels (Maslin, 2009), thus the Amazon Fan, much like the Amazon River, is highly sensitive to changes in sea level.

The modern onshore Amazon system is fairly well-constrained by existing detrital geochronology (Fig. 1A, B) (Mapes, 2009; Iizuka et al., 2010). DZ age data from the main stem Solimões and lower Amazon River display a progressive dilution of Andean age modes (<1.3 Ga) by older Amazon Craton age modes (Fig 1B). The observed pattern of downstream dilution by older cratonic sources might predict a DZ age spectra in the submarine fan dominated by cratonic signatures. Here, we use DZ samples from the Amazon Fan to constrain the provenance signature of the most distal segment of the system, in order to test hypotheses related to multi-millennial timescale sediment transfer dynamics in Earth's largest fluvial to deep-sea network.

METHODS AND RESULTS

We collected 10 samples of upper fine- to medium-grained sand from turbidite beds in cores recovered during ODP Leg 155, Sites 936, 945, and 946 in the lower Amazon Fan (Fig 1A for locations; Supplementary Data File 1). All sample preparation, analyses, and data reduction were conducted at the UTChron facility at the University of Texas at Austin, where we used standard techniques of mineral separation, and applied laser ablation inductively coupled plasma-mass spectrometry U-Pb dating to zircon grains (methods of Thompson et al., 2017, and references therein).

Resultant DZ ages are presented within their composite stratigraphic context (Fig. 2A) as kernel density estimates (KDE; Fig. 2B, 2C), and plotted using a multidimensional scaling map

(MDS map; Fig. 2D). Full isotopic results are reported in Supplementary Data File 2. DZ age modes present in the Amazon Fan (Fig. 2C), from youngest to oldest include Eocene-Oligocene (ca. 30 Ma), minor Jurassic (ca. 174 Ma), major bimodal Triassic-Permian (ca. 252 and 310 Ma, respectively), a complex Pan-African or Brasiliano signature (ca. 534, 612, and 788 Ma), major bimodal Sunsas (ca. 1038 and 1170 Ma), minor Rondonian-San Ignacaio (ca. 1530 Ma), a well-distributed mode across ca. 1700 – 2200 Ma with less prominent Venturai Tapajos (ca. 1880 Ma), and a handful of grains with ages > 2200 Ma.

Individual sample KDEs displayed in Figure 2B show little evidence of systematic variability in space or time. Minor inter-sample variability is marked by differences in proportions of Phanerozoic and Pan African-Brasiliano age modes (see Supplementary Figure 1). However, the mean and standard deviation (1σ) of KDE cross-correlation coefficients for all Amazon Fan samples is 0.45 ± 0.08 (see Supplementary table 2), which is consistent with, or slightly less than coefficients for synthetic subsamples drawn from the same parent sample (Saylor and Sundell, 2016).

Collectively, Amazon Fan DZ samples (Fig. 2C) have nearly identical age modes as published samples from the onshore Amazon system (Mapes, 2009; Iizuka et al., 2010) (Fig. 2C). However, two distinctions may be made: (1) fan samples are qualitatively more homogenous than modern samples from the length of Amazon River, which display high spatial variability (Mapes, 2009), and (2) Amazon Fan DZ age spectra are dissimilar to the lower Amazon DZ age spectra (Figs. 1B, 2D), which are dominated by cratonic grains (52% U-Pb ages >1.3 Ga) (See supplementary Table 1). Thus, contrary to indications that Amazon Fan age spectra should resemble the lower Amazon, our data show that Amazon Fan age spectra are

nearly identical to the age spectra generated by integrating samples from the length of the modern mainstem Amazon River.

DISCUSSION

Consistent DZ age distributions from the Amazon Fan could be the result of a relatively stable Pleistocene Amazon hydroclimate (Novello et al., 2017), or alternatively may relate to sediment storage, recycling, and mixing within floodplains and the coastal zone (Meade, 1985; Dunne et al, 1998). Cosmogenic radionuclides from the modern Amazon River suggest significant onshore storage and recycling of sediment en route to the coast (Wittmann et al., 2011). As noted by others, the enormous sediment trapping capacity of the lower Amazon River at high sea level must have been significantly reduced during the LGM and previous global glacioeustatic lowstands (between MIS 12 or 8 – MIS 2; Lisiecki and Raymo, 2005), when incision lead to increased channel gradients along at least 1200 km of the lower Amazon (Mertes and Dunne, 2007).

We hypothesize that base level (sea level) controls the DZ age signatures in the Amazon River-to-fan system. During highstands, sediment storage in lowland floodplains and the coastal zone results in dilution of younger Andean DZs by older cratonic grains from subcatchments proximal to the lower reaches of the Amazon River. Then, during falling through early transgressive phases, a lower base level results in a steepened Amazon River profile, decreased sediment retention in tributary and main stem floodplains, and recycling and evacuation of the river valley and coastal zone deposits. These processes would coincide with channel lengthening (*sensu* Blum and Törnqvist, 2000), more efficient transfer of upland-sourced (Andean) sediment

160 to the submarine fan, causing the observed integrated DZ signature, rather than the craton-
161 dominated DZ signature of sediment from the modern lower Amazon River.
162 Results from the Pleistocene Amazon Fan contrast with similar data sets from other
163 major land-to-sea sediment routing systems that emphasize an up-system climate driver of
164 provenance variability rather than base level. The late Pleistocene Mississippi catchment
165 experienced significant modifications to extents and hydrology due to ice-sheet activity, which
166 lead to a climatic modulation of the Missouri-Mississippi River System throughput to the
167 Mississippi Fan (Fildani et al., 2016), and sediment mixing in the coastal zone did not
168 significantly dampen distant climate signals. In the Indus source-to-sink system, variable
169 monsoonal intensity since the LGM resulted in measurable changes in provenance of sediment
170 from cores along the delta (Clift et al., 2008; Clift and Giosan, 2013). The degree to which
171 upstream changes in sediment sources may have influenced downstream mixtures of DZs in the
172 Amazon Fan is an interesting problem that merits further examination (*e.g.* Mason et al., 2017).
173 Yet because the Amazon catchment straddles a relatively stable climate zone (Novello et al.,
174 2017), we posit that sea level plays a first-order control on the observed sediment dynamics in
175 the Amazon river-to-fan system.
176 The influence of sea-level changes on sediment supply to the Amazon Fan has been well
177 documented (summarized by Maslin, 2009), and has been formally conceptualized in other
178 systems globally (Blum and Tornqvist, 2000; Blum and Hattier-Womack, 2009). Our data set of
179 DZ from the Amazon River and Fan offers insights into the influence of base level on the
180 system-scale (river-to-sea) functioning of Earth's largest sediment routing system. Finally, we
181 note that while high-frequency (~10^4 yr) signals of upstream environmental change might have
182 been dampened by sediment storage and recycling in floodplains or coastal zones of such large

tropical/greenhouse sediment routing systems, their submarine fans should preserve high-fidelity records of large-scale drainage reorganizations, major climate-regime fluctuations, or tectonic perturbations over 10^6 yr timescales.

CONCLUSIONS

The Pleistocene Amazon submarine fan archives a record of sediment transferred from the South American continent to the deep sea. Detrital U-Pb zircon geochronology (DZ; N = 10 samples, n = 1,362 grains) from the submarine fan show little systematic variation across 100s m of strata, and across ~10^5 yr timescales, suggesting that either the climate system in the tropics does not sufficiently perturb sediment loads from tributaries to the Amazon, or that the Amazon system efficiently buffers changes in sediment source composition via storage and subsequent mixing of sediment en route to the submarine fan. The strong resemblance of Pleistocene fan samples to a modern catchment-integrated DZ signature, rather than the lower Amazon DZ signature, suggests a significant decrease of sediment retention in floodplains during sea-level lowstands, which results in enhanced sediment throughput from the upper Amazon and its tributaries to the linked submarine fan.

ACKNOWLEDGEMENTS

Funding for analyses and CM's postdoctoral fellowship was provided by Statoil. Lisa Stockli provided assistance in the laboratory, and Ken Eriksson provided helpful discussions. We thank XX reviewers for helpful comments.

FIGURE CAPTIONS

Figure 1: Physiography and simplified detrital zircon (DZ) source terrane map of the Amazon catchment and submarine fan system **A**: Major fluvial elements of the Amazon River system, existing onshore detrital zircon (DZ) sample locations from Mapes (2009), except where labeled IZ = Iizuka et al., (2010), locations of Ocean Drilling Program (ODP) sediment cores used in this study. Geology from Chew et al. (2011) and references therein. **B**: Pie diagrams of DZ age spectra from the upper Amazon vs. lower Amazon. For associated fractions see Supplementary Table 1.

Figure 2: Results of U-Pb detrital zircon (DZ) geochronology from the Amazon submarine fan. **A**: composite stratigraphic section from Ocean Drilling Program (ODP) Leg 155, Sites 936-2, 945-1, and 946-6 (after Damuth et al., 1995), with interpreted ages of strata, marine isotope stages (MIS) and schematic DZ sample locations. **B**: kernel density estimates (KDEs) from samples in A. **C**: Amalgamated U-Pb DZ geochronology from the Amazon submarine fan, binned at 25 Myr intervals, and compared to amalgamated DZ samples from the Amazon River (Mapes, 2009; Iizuka et al., 2010). Annotations in italics denote ages of bins rather than KDE peaks. **D**: Multidimensional scaling map (MDS) of samples from the Amazon submarine fan and fluvial network (Vermeesch, 2013).

REFERENCES

Aalto, R., Dunne, T., Guyot, J.L., 2006. Geomorphic Controls on Andean Denudation Rates. J. Geol. 114, 85–99. doi:10.1086/498101

228 Amidon, W.H., Burbank, D.W., Gehrels, G.E., 2005. Construction of detrital mineral
229 populations: insights from mixing of U-Pb zircon ages in Himalayan rivers. Basin Res. 17,
230 463–485. doi:10.1111/j.1365-2117.2005.00279.x
231 Blum, M.D., Hattier-Womack, J., 2009. Climate Change, Sea-Level Change, and Fluvial
232 Sediment Supply to Deepwater Depositional Systems. Extern. Control. Deep. Depos. Syst.
233 92, 15–39. doi:10.2110/sepmsp.092.015
234 Blum, M.D., Törnqvist, T.E., 2000. Fluvial responses to climate and sea-level change: a review
235 and look forward. Sedimentology 47, 2–48. doi:10.1046/j.1365-3091.2000.00008.x
236 Blum, M., Rogers, K., Gleason, J., Najman, Y., Cruz, J., Fox, L., 2018. Allogenic and Autogenic
237 Signals in the Stratigraphic Record of the Deep-Sea Bengal Fan. Sci. Rep. 1–13.
238 doi:10.1038/s41598-018-25819-5
239 Chew, D.M., Cardona, A., Mišković, A., 2011. Tectonic evolution of western Amazonia from
240 the assembly of Rodinia to its break-up. Int. Geol. Rev. 53, 1280–1296.
241 doi:10.1080/00206814.2010.527630
242 Clift, P.D., Giosan, L., 2014. Sediment fluxes and buffering in the post-glacial Indus Basin.
243 Basin Res. 26, 369–386. doi:10.1111/bre.12038
244 Clift, P.D., Giosan, L., Blusztajn, J., Campbell, I.H., Allen, C., Pringle, M., Tabrez, A.R.,
245 Danish, M., Rabbani, M.M., Alizai, A., Carter, A., Lückge, A., 2008. Holocene erosion of
246 the Lesser Himalaya triggered by intensified summer monsoon. Geology 36, 79–82.
247 doi:10.1130/G24315A.1
248 Covault, J.A., Graham, S.A., 2010. Submarine fans at all sea-level stands: Tectono-morphologic
249 and climatic controls on terrigenous sediment delivery to the deep sea. Geology 38, 939–
250 942. doi:10.1130/G31081.1

Damuth, J.E., Flood, R.D., Pirmez, C., and Manley, P.L., 1995, Architectural elements and depositional processes of Amazon Deep-sea Fan imaged by long-range sidescan sonar (GLORIA), bathymetric swath-mapping (Sea Beam), high-resolution seismic and piston-core data, in Pickering, K.T., Hiscott, R.N., Kenyon, N.H., Ricci Lucchi, F., and Smith, R.D.A., eds., Atlas of Deep Water Environments; Architectural Style in Turbidites : Oxford, U.K., Chapman & Hall, p. 105-121.

Dunne, T., Mertes, L.A.K., Meade, R.H., Richey, J.E., Forsberg, B.R., 1998. Exchanges of sediment between the flood plain and channel of the Amazon River in Brazil. Bull. Geol. Soc. Am. 110, 450–467. doi:10.1130/0016-7606(1998)110<0450:EOSBTF>2.3.CO;2

Figueiredo, J., Hoorn, C., van der Ven, P., Soares, E., 2009. Late Miocene onset of the Amazon River and the Amazon deep-sea fan: Evidence from the Foz do Amazonas Basin. Geology 37, 619–622. doi:10.1130/G25567A.1

Fildani, A., McKay, M.P., Stockli, D., Clark, J., Dykstra, M.L., Stockli, L., Hessler, A.M., 2016. The ancestral Mississippi drainage archived in the late Wisconsin Mississippi deep-sea fan. Geology 44, 479–482. doi:10.1130/G37657.1

Fisk, H.N., 1944. Geological investigation of the alluvial valley of the lower Mississippi River. Mississippi River Commission, Vicksburg, Mississippi.

Iizuka, T., Komiya, T., Rino, S., Maruyama, S., Hirata, T., 2010. Detrital zircon evidence for Hf isotopic evolution of granitoid crust and continental growth. Geochim. Cosmochim. Acta 74, 2450–2472. doi:10.1016/j.gca.2010.01.023

Lisiecki, L.E., Raymo, M.E., 2005. A Pliocene-Pleistocene stack of 57 globally distributed benthic δ18O records. Paleoceanography 20, 1–17. doi:10.1029/2004PA001071

Mapes, R.W., 2009, Past and present provenance of the Amazon River drainage basin [Ph.D. thesis]: University of North Carolina.

Maslin, M., 2009. Review of the Timing and Causes of the Amazon-Fan Mass Transport and Avulsion Deposits During the Latest Pleistocene. Extern. Control. Deep. Depos. Syst. 92, 133–144. doi:10.2110/sepmsp.092

Mason, C.C., Fildani, A., Gerber, T., Blum, M.D., Clark, J.D., Dykstra, M., 2017. Climatic and anthropogenic influences on sediment mixing in the Mississippi source-to-sink system using detrital zircons: Late Pleistocene to recent. Earth Planet. Sci. Lett. 466, 70–79. doi:10.1016/j.epsl.2017.03.001

Meade, R.H., Dunne, T., Richey, J.E., Santos, U., Salati, E., 1985. Storage and remobilization of suspended sediment in the lower Amazon river of Brazil. Science. doi:10.1126/science.228.4698.488

Meade, R.H., Rayol, J.M., Conceição, S.C. Da, Natividade, J.R.G., 1991. Backwater Effects in the Amazon River of Basin. Environ. Geol. Water Sci. 18, 105–114. doi:10.1007/BF01704664

Mertes, L.A.K., Dunne, T., 2007. Effects of Tectonism, Climate Change, and Sea-level Change on the Form and Behaviour of the Modern Amazon River and its Floodplain, Large Rivers: Geomorphology and Management. doi:10.1002/9780470723722.ch8

Milliman, J. D. & Farnsworth, K. L. River Discharge to the Coastal Ocean: A Global Synthesis (Cambridge Univ. Press, 2011)

Müller, J., Irion, G., Nunes de Melho, J., and Junk, W.J., 1995, Hydrological changes of the Amazon during the last glacial-interglacial cycle in central Amazonia (Brazil), aturwissenschaften, v. 82, pp. 232–235.

296 Nittrouer, C.A., Kuehl, S.A., Demaster, D.J., Kowsmann, R.O., 1986. The deltaic nature of
297 Amazon shelf sedimentation. Geol. Soc. Am. Bull. 97, 444–458. doi:10.1130/0016-
298 7606(1986)97<444:TDNOAS>2.0.CO;2
299 Normark, W.R., Reid, J.A., 2003. Extensive Deposits on the Pacific Plate from Late Pleistocene
300 North American Glacial Lake Outbursts. J. Geol. 111, 617–637. doi:10.1086/378334
301 Novello, V.F., Cruz, F.W., Vuille, M., Stríkis, N.M., Edwards, R.L., Cheng, H., Emerick, S., De
302 Paula, M.S., Li, X., Barreto, E.D.S., Karmann, I., Santos, R. V., 2017. A high-resolution
303 history of the South American Monsoon from Last Glacial Maximum to the Holocene. Sci.
304 Rep. 7, 1–8. doi:10.1038/srep44267
305 Saucier, R.T., 1996. A contemporary appraisal of some key Fiskian concepts with emphasis on
306 Holocene meander belt formation and morphology. Engineering Geol. 45, 67–86.
307 Saylor, J.E., Knowles, J.N., Horton, B.K., Nie, J., Mora, A., 2013. Mixing of Source Populations
308 Recorded in Detrital Zircon U-Pb Age Spectra of Modern River Sands. J. Geol. 121, 17–33.
309 doi:10.1086/668683
310 Saylor, J.E., Sundell, K.E., 2016. Quantifying comparison of large detrital geochronology data
311 sets. Geosphere 12, 203–220. doi:10.1130/GES01237.1
312 Sickmann, Z.T., Paull, C.K., Graham, S.A., 2016. Detrital-zircon mixing and partitioning in
313 fluvial to deep marine systems, central California, U.S.A.. J. Sediment. Res. 86, 1298–1307.
314 Sweet, M.L., Blum, M.D., 2016. Connections Between Fluvial To Shallow Marine Environments
315 and Submarine Canyons: Implications for Sediment Transfer To Deep Water. J. Sediment.
316 Res. 86, 1147–1162. doi:10.2110/jsr.2016.64
317 Thomson, K.D., Stockli, D.F., Clark, J.D., Puigdefàbregas, C., Fildani, A., 2017. Detrital zircon
318 (U-Th)/(He-Pb) double-dating constraints on provenance and foreland basin evolution of

the Ainsa Basin, south-central Pyrenees, Spain. Tectonics 36, 1352–1375. doi:10.1002/2017TC004504

Vermeesch, P., 2013. Multi-sample comparison of detrital age distributions. Chem. Geol. 341, 140–146. doi:10.1016/j.chemgeo.2013.01.010

Wittmann, H., von Blanckenburg, F., Maurice, L., Guyot, J.L., Filizola, N., Kubik, P.W., 2011. Sediment production and delivery in the Amazon River basin quantified by in situ-produced cosmogenic nuclides and recent river loads. Bull. Geol. Soc. Am. 123, 934–950. doi:10.1130/B30317.1

Figure 1

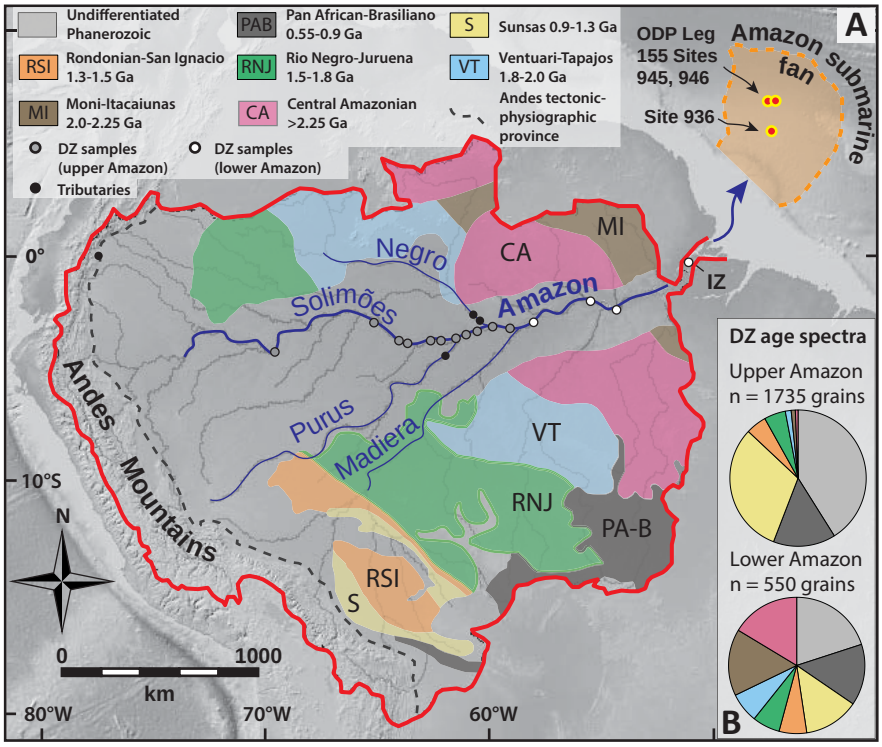
Undifferentiated Phanerozoic
PAB Pan African-Brasiliano 0.55-0.9 Ga
S Sunsas 0.9-1.3 Ga
RSI Rondonian-San Ignacio 1.3-1.5 Ga
RNJ Rio Negro-Juruena 1.5-1.8 Ga
VT Ventuari-Tapajos 1.8-2.0 Ga
MI Moni-Itacaiunas 2.0-2.25 Ga
CA Central Amazonian >2.25 Ga
Andes tectonic-physiographic province
DZ samples (upper Amazon)
DZ samples (lower Amazon)
Tributaries
ODP Leg 155 Sites 945, 946
Site 936
Amazon submarine fan
A
Negro
Solimões
Amazon
Purus
Madiera
Andes Mountains
MI
CA
IZ
VT
RNJ
PA-B
RSI
S
0°
10°S
N
0
1000
km
80°W
70°W
60°W
DZ age spectra
Upper Amazon
n = 1735 grains
Lower Amazon
n = 550 grains
B

Figure 2

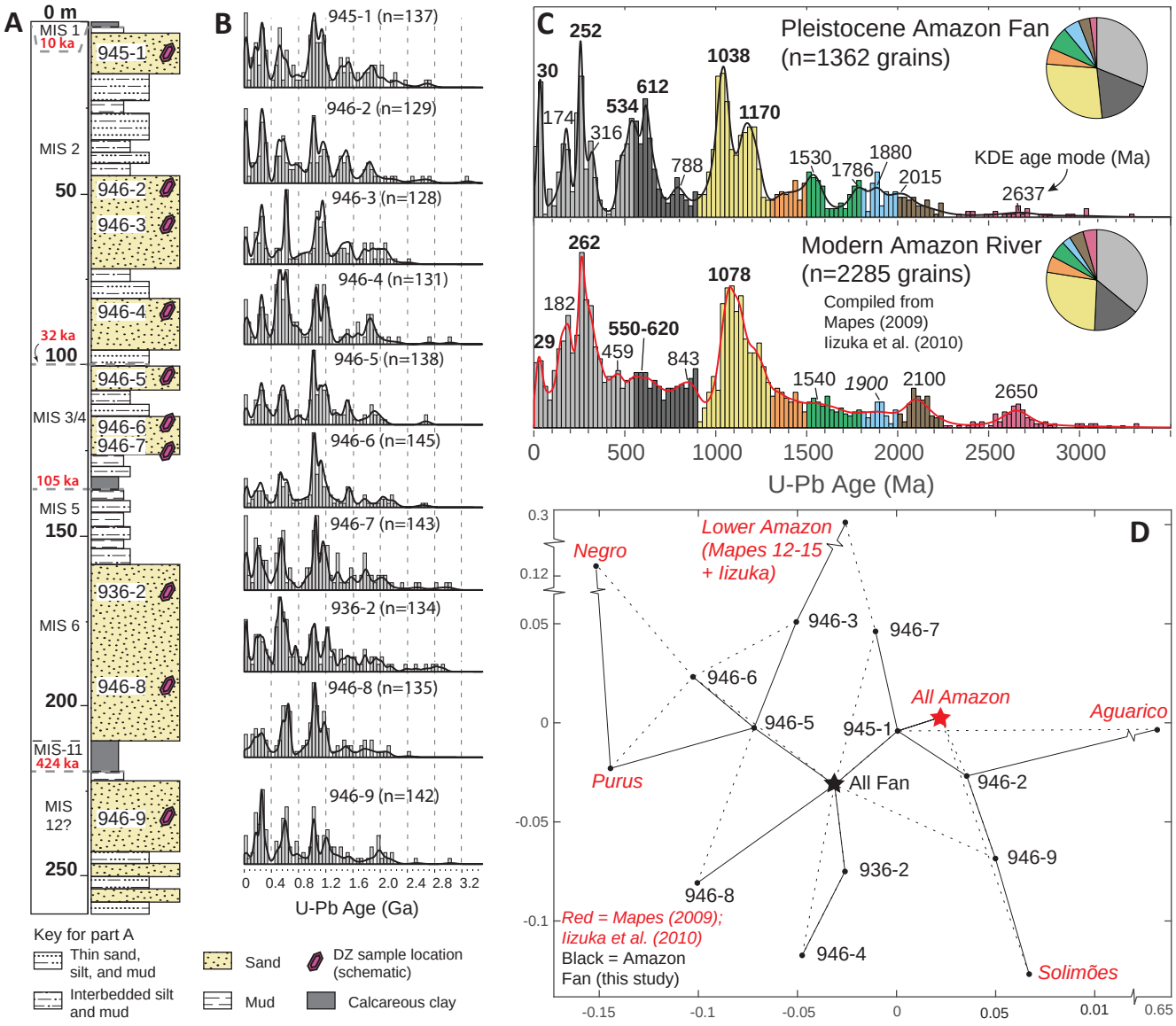
A
0 m
MIS 1
10 ka
945-1
MIS 2
50
946-2
946-3
946-4
32 ka
100
946-5
MIS 3/4
946-6
946-7
105 ka
MIS 5
150
936-2
MIS 6
946-8
200
MIS-11
424 ka
MIS 12?
946-9
250
B
945-1 (n=137)
946-2 (n=129)
946-3 (n=128)
946-4 (n=131)
946-5 (n=138)
946-6 (n=145)
946-7 (n=143)
936-2 (n=134)
946-8 (n=135)
946-9 (n=142)
0 0.4 0.8 1.2 1.6 2.0 2.4 2.8 3.2
U-Pb Age (Ga)
C
Pleistocene Amazon Fan
(n=1362 grains)
252
30
174
316
534
612
788
1038
1170
1530
1786
1880
2015
2637
KDE age mode (Ma)
Modern Amazon River
(n=2285 grains)
Compiled from
Mapes (2009)
Iizuka et al. (2010)
262
182
29
459
550-620
843
1078
1540
1900
2100
2650
0 500 1000 1500 2000 2500 3000
U-Pb Age (Ma)
D
Negro
Lower Amazon
(Mapes 12-15
+ Iizuka)
946-3
946-7
946-6
All Amazon
Aguarico
946-5
945-1
Purus
All Fan
946-2
946-9
936-2
946-8
946-4
Solimões
Red = Mapes (2009);
Iizuka et al. (2010)
Black = Amazon
Fan (this study)
0.3
0.12
0.05
0
-0.05
-0.1
-0.15 -0.1 -0.05 0 0.05 0.01 0.65
Key for part A
Thin sand, silt, and mud
Interbedded silt and mud
Sand
Mud
DZ sample location (schematic)
Calcareous clay

Description of Supplementary Materials for "*Detrital Zircons from the Amazon river-to-fan system reveal base level controls on land-to-sea sediment transfer*"

The supplementary materials consist of two tables, two data files and one figure.

Contents

i. Supplementary Table 1: Fractions of DZ ages across the onshore and offshore Amazon system (this document)

ii. Supplementary Data File 1: ODP Amazon fan Samples (.xlsx) not included in preprint

iii. Supplementary Data File 2: Amazon DZ DATA (.xlsx) not included in preprint

iv. Supplementary Figure 1: kernel density estimates (KDEs) and cumulative distribution functions (CDFs) for detrital zircon samples from the Amazon Fan (this document)

v. Supplementary Table 2: Cross correlation coefficients for detrital zircon samples from the Amazon Fan (this document)

Supplementary Table 1: Fractions of DZ ages across the onshore and offshore Amazon system

Age grouping (Ma)	Upper onshore Amazon (Mapes *1-12) (%)	Lower onshore Amazon (Mapes 13-15 + Iizuka) (%)	All onshore (%)	All fan (%)
<550	41	20	36	31
550-950	15	15	15	17
950-1300	31	13	27	28
1300-1500	5	7	5	5
1500-1800	5	7	5	7
1800-2000	1	7	3	5
2000-2250	1	16	5	4
>2250	1	16	4	2

*See Mapes (2009) for reference to Sample numbers

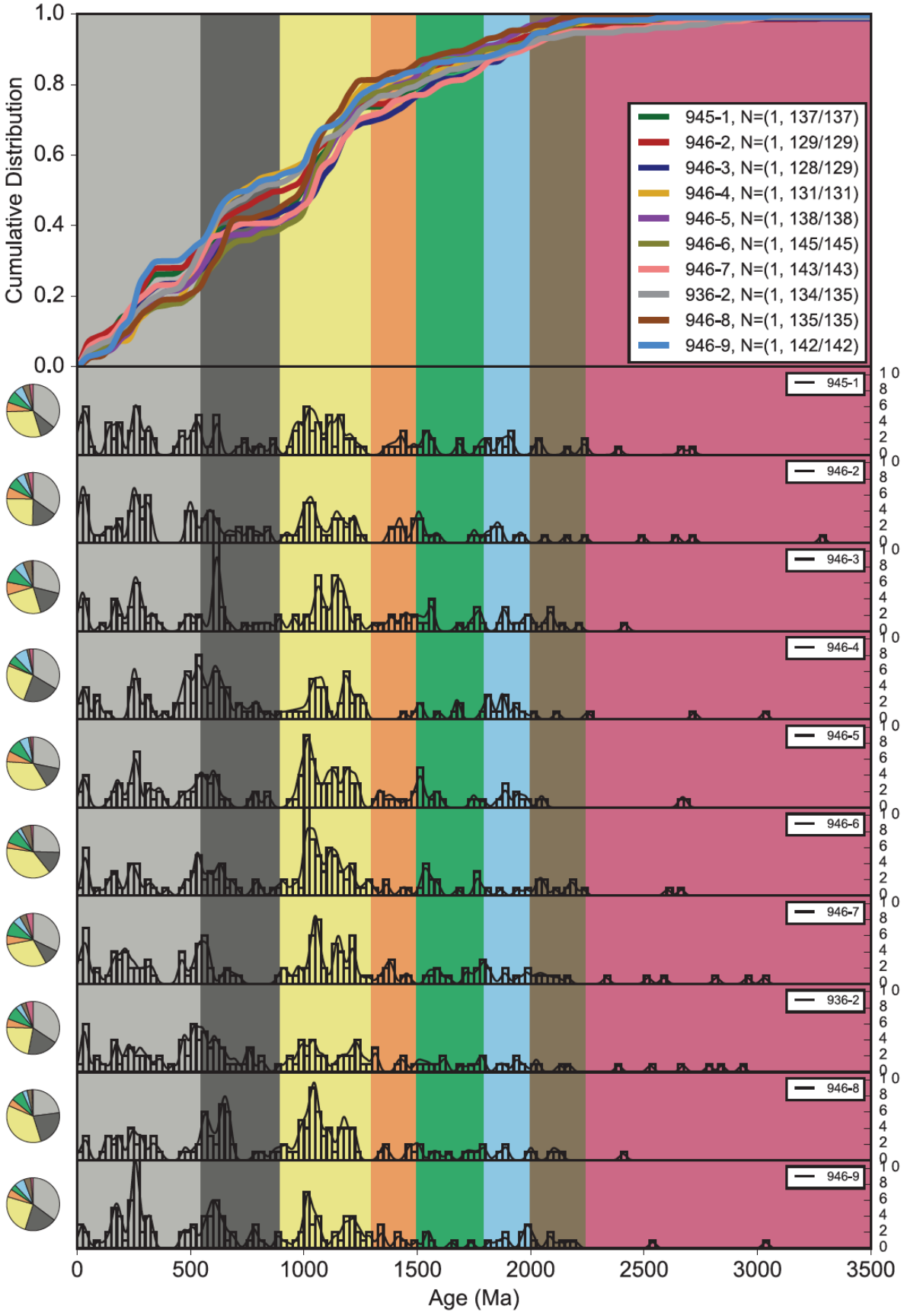
Cumulative Distribution
1.0
0.8
0.6
0.4
0.2
0.0
945-1, N=(1, 137/137)
946-2, N=(1, 129/129)
946-3, N=(1, 128/129)
946-4, N=(1, 131/131)
946-5, N=(1, 138/138)
946-6, N=(1, 145/145)
946-7, N=(1, 143/143)
936-2, N=(1, 134/135)
946-8, N=(1, 135/135)
946-9, N=(1, 142/142)
945-1
946-2
946-3
946-4
946-5
946-6
946-7
936-2
946-8
946-9
0
500
1000
1500
2000
2500
3000
3500
Age (Ma)

Supplementary Figure 1: Cumulative distribution functions, pie charts, and kernel density estimates for all Amazon Fan U-Pb detrital zircon data used in the main text. U-Pb ages binned at 25 Myr intervals.

Supplementary Table 2: Cross-correlation of kernel density estimation
(after Saylor and Sundell, 2016)

sample	# grains (n)	945-1	946-2	946-3	946-4	946-5	946-6	946-7	936-2	946-8	946-9
945-1	137	1	0.584	0.517	0.389	0.588	0.610	0.450	0.413	0.369	0.494
946-2	129	0.584	1	0.401	0.433	0.605	0.451	0.382	0.446	0.378	0.551
946-3	129	0.517	0.401	1	0.402	0.425	0.401	0.313	0.319	0.346	0.488
946-4	131	0.389	0.433	0.402	1	0.422	0.394	0.332	0.536	0.411	0.440
946-5	138	0.588	0.605	0.425	0.422	1	0.641	0.405	0.474	0.530	0.575
946-6	145	0.610	0.451	0.401	0.394	0.641	1	0.526	0.433	0.565	0.414
946-7	143	0.450	0.382	0.313	0.332	0.405	0.526	1	0.441	0.497	0.322
936-2	135	0.413	0.446	0.319	0.536	0.474	0.433	0.441	1	0.391	0.401
946-8	135	0.369	0.378	0.346	0.411	0.530	0.565	0.497	0.391	1	0.445
946-9	142	0.494	0.551	0.488	0.440	0.575	0.414	0.322	0.401	0.445	1